Work-in-Progress

Localization of Motor Areas Adjacent to Arteriovenous Malformations

A Positron Emission Tomographic Study

Scott T. Grafton, MD
Division of Nuclear Medicine and Biophysics
Departments of Neurology and Radiology
University of California, Los Angeles (UCLA) School of Medicine
Los Angeles, CA

Neil A. Martin, MD
Division of Neurosurgery
UCLA School of Medicine

John C. Mazziotta, MD, PhD
Division of Nuclear Medicine and Biophysics
Departments of Neurology and Radiology
UCLA School of Medicine

Roger P. Woods, MD
Department of Neurology
UCLA School of Medicine

Fernando Vinuela, MD
Department of Radiology
UCLA School of Medicine

Michael E. Phelps, PhD
Division of Nuclear Medicine and Biophysics
Department of Radiology
UCLA School of Medicine and Laboratory of Nuclear Medicine
U.S. Department of Energy

ABSTRACT

Motor cortex activity was localized with positron emission tomography (PET) in 4 patients with large arteriovenous malformations adjacent to or undercutting the left primary motor cortex. Relative cerebral blood flow responses were measured during execution of a visually guided motor tracking task performed with the right index finger, hand, great toe, tongue, or eyes alone (control) and mapped onto each patient's corresponding magnetic resonance imaging (MRI) scan. The relative cerebral blood flow responses in the contralateral precentral gyrus, adjacent to each arteriovenous malformation, demonstrated a normal somatotopic distribution, similar to that in a control population. In the 3 patients with preserved motor function, responses were also present in the ipsilateral primary motor cortex, bilateral supplementary motor area, and ipsilateral anterior cerebellum, similar in location to those of a control population. In the fourth patient with a hemiparesis, responses were attenuated in the primary motor cortex, increased in the supplementary motor area, and absent in the cerebellum. The results demonstrate that PET cerebral blood flow mapping can localize motor cortex despite the presence of significant blood flow abnormalities in adjacent arteriovenous malformations. The method, particularly when combined with MRI, may be used in the planning of surgical, radiation, or embolization therapy.

Grafton ST, Martin NA, Mazziotta JC, Woods RP, Vinuela F, Phelps ME. Localization of motor areas adjacent to arteriovenous malformations: a positron emission tomographic study. J Neuroimag 1994;4:97–103

Received Jul 14, 1993, and in revised form Oct 25. Accepted for publication Oct 26, 1993.

Address correspondence to Dr Grafton, Departments of Neurology and Radiology, University of Southern California, HCC 350, 1510 San Pablo Street, Los Angeles, CA 90033-4606.

The risk of mortality or neurological morbidity from arteriovenous malformation (AVM) rupture is substantial [1]. Therefore it has been recommended that all patients with AVMs be evaluated for possible surgical treatment [1–3]. A key factor in determining the risk of neurological morbidity is the anatomical relationship of the malformation to functionally important regions of the cortex [2]. The integrity and functional significance of the adjacent cortex can be assessed by a number of invasive methods [4]. For example, intraoperative cortical stimulation has been used to map language, motor, and sensory areas in awake patients [5, 6]. In anesthetized patients, electrical potentials of the postcentral gyrus can be monitored during peripheral sensory stimulation [6, 7]. Nevertheless, these techniques do not provide a noninvasive method that can be employed preoperatively for the prediction of surgical risk.

Preoperatively, superselective angiography combined with amobarbital (Amytal) infusion and neurobehavioral testing provides an alternative technique for assessing awake patients [8, 9]. Although this is more precise than hemispheric amobarbital (Wada) testing, the vascular territory evaluated may still be too broad to permit precise functional localization. Furthermore, false-negative results are possible when the amobarbital shunts through the AVM and does not reach the adjacent parenchyma. Magnetic resonance imaging (MRI) has been used to identify the central sulcus and adjacent precentral gyrus (primary motor cortex) [10]. This localizing technique may be difficult to use when the sulcal anatomy is distorted or obscured by a large cortical AVM. Alternatively, positron emission tomography (PET) has been used to map the somatosensory cortex in a patient with a perirolandic AVM [11]. In that patient, vibrotactile stimulation was used to define the postcentral gyrus located in proximity to a frontoparietal AVM.

This report describes a preoperative PET method for non-

invasive functional mapping of motor areas. Four patients with AVMs adjacent to or undercutting the left precentral gyrus were examined. Each performed a series of motor tracking tasks with either the right index finger, arm, leg, tongue, or eyes alone (control) during PET imaging. This technique allows selective mapping of primary motor areas controlling specific movements, and of secondary motor areas.

Methods and Subjects

Imaging: Serial images of relative (rel) cerebral blood flow (CBF) were obtained with PET in 12 normal subjects and 4 patients with AVMs while they each performed a set of motor tracking tasks. Each subject received from three to six sequential intravenous bolus injections of 50 mCi of radioactive water ($H_2{}^{15}O$) commensurate with dynamic PET imaging with the Siemens/CTI 831 tomograph (Siemens, Hoffman Estate, IL). The tomograph collects 15 continuous planes of 6.75-mm thickness and with an in-plane resolution of 6 mm. Final image resolution after reconstruction was smoothed to 13-mm of full width at half maximum. Emission images were corrected for attenuation using a transmission ring source of germanium 68 collected in the same head position. Head immobilization was maintained with a custom foam mold (Smithers, Akron, OH).

Estimates of relCBF were based on a modified autoradiographic method [12, 13]. Five-second scan frames were collected for 2 minutes. Data from 70 seconds of these frames were summed, beginning with the first frame showing the tracer arrival in the brain, to generate relCBF images. Arterial blood sampling was not performed so that the subjects would have an untethered arm to perform the motor tasks. Therefore, the final images represented relative images of tissue activity rather than absolute estimates of regional blood flow. Images such as these demonstrate a near linear relationship to actual CBF in normal subjects and provide a reasonable estimate of local CBF [14, 15]. It was assumed that a similar relationship exists in patients with AVMs, based on findings from a previous quantitative study [16].

Subjects: All patients and normal volunteers were studied after giving informed consent in accordance with the University of California, Los Angeles (UCLA) Human Subject Protection Committee. Twelve normal subjects (mean age, 23 yr [standard deviation, 1.5]; 11 male, 1 female; 10 right-handed, 2 left-handed) were studied as previously described [17, 18]. All were drug free, were without any history of nervous system disease or injury, and demonstrated normal findings on examination. Four patients with large (>5 cm in diameter) AVMs situated adjacent to the left motor cortex were examined. Five of the normal subjects and all 4 patients also underwent MRI with an inversion recovery protocol (TR 1275/TE 30/TI 300) that generated 15 to 30 contiguous planes of data with an interslice distance of 4.4 mm and in-plane resolution of 1 mm (Fonar Systems, 0.35 T, Melville, NY; or General Electric Signa, 1.5 T, Milwaukee, WI).

Patient Histories: Patient 1 was a 22-year-old right-handed man with a left frontal AVM located anterior to the precentral gyrus (Fig 1A). The patient had no motor deficit. PET scans were obtained prior to selective embolization, intraoperative mapping of sensory motor cortex using cortical recording of somatosensory evoked potentials (SSEPs), and complete resection of the malformation. Postoperatively, the patient developed transient language deficit and right hemiparesis, which resolved completely over 4 weeks.

Patient 2, a 28-year-old right-handed man, had a deep AVM undercutting the middle and superior portions of the left precentral gyrus (see Fig 1B). The patient was normal on neurological examination. PET scans were obtained prior to any intervention. Superselective angiography and amobarbital injection in the area of the AVM demonstrated impairment of hand motor function when the AVM was perfused. Because of the apparent proximity of the AVM to primary motor cortex as demonstrated by MRI and the results of the amobarbital injection, the patient was treated with stereotaxic radiosurgery using a linear accelerator. At the time of writing, the patient remained normal neurologically.

Patient 3, a 21-year-old left-handed woman, had a left frontal AVM located within the dorsal precentral gyrus and extending into the frontal lobe (see Fig 1C). She had a gradually progressive, mild spastic weakness involving the right leg. The patient underwent intraoperative cortical recording of SSEPs to localize sensory motor cortex. Because the AVM involved primary motor cortex, intraoperative embolization rather than excision was elected. After the procedure the patient had transient worsening of the leg weakness, which gradually returned to baseline status. Stereotaxic radiosurgery is planned to treat the residual malformation. Postoperative PET scans were obtained after return to baseline status.

Patient 4, a 22-year-old right-handed woman, had an extensive left frontal AVM located within the dorsal precentral gyrus extending inferior to the insula and inferior left frontal lobe (see Fig 1D). She had a gradually progressive right hemiparesis affecting the arm more than the leg. In addition, she had recurrent episodes of transient right arm weakness, greater than at baseline, that were hypothesized to be secondary to a steal phenomenon associated with the AVM. PET was performed prior to any intervention and during a period of significant arm weakness. Because of the proximity of the AVM to motor and language cortex, only palliative embolization to reduce steal was recommended.

Tasks: Subjects performed a set of motor tasks in response to a simple target stimulus presented on a 13-in video mon-

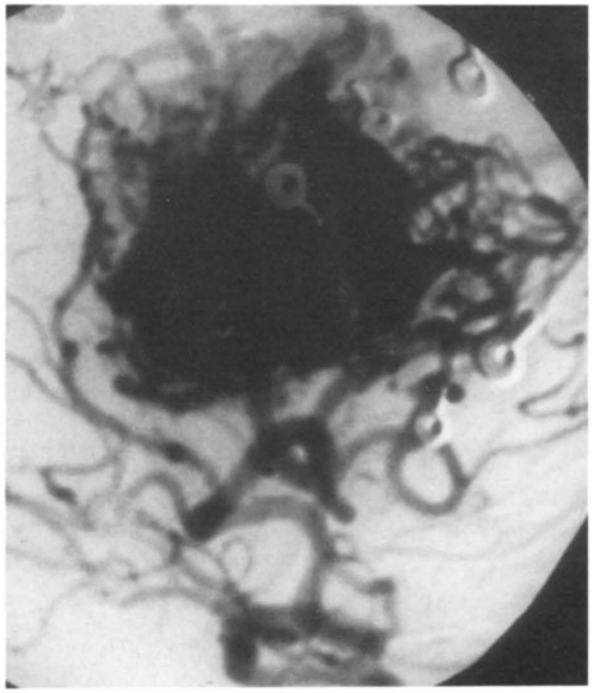

A

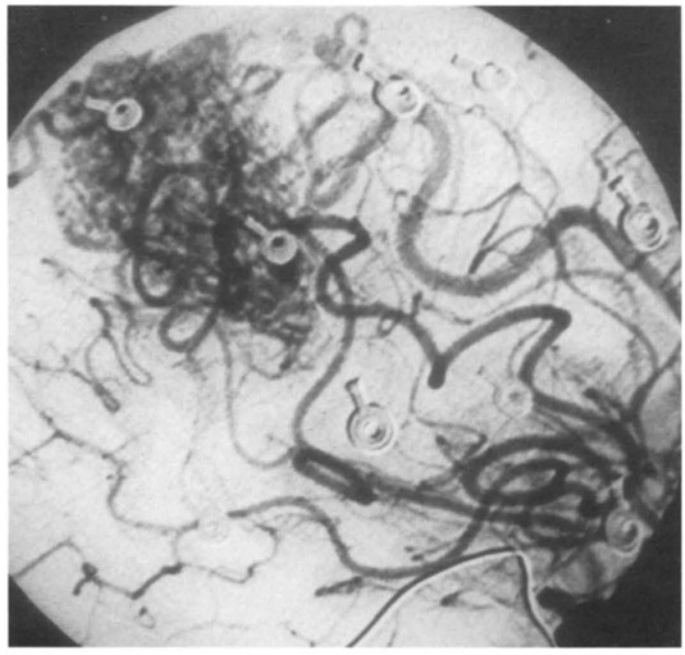

C

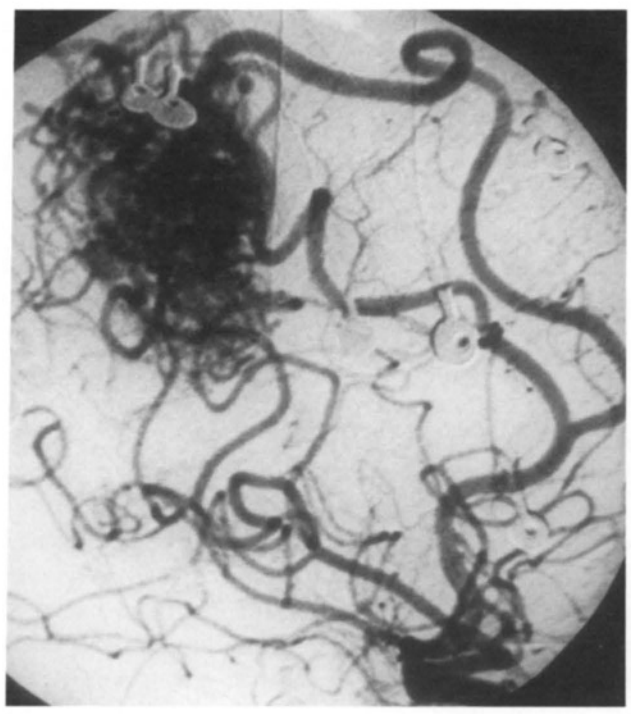

B

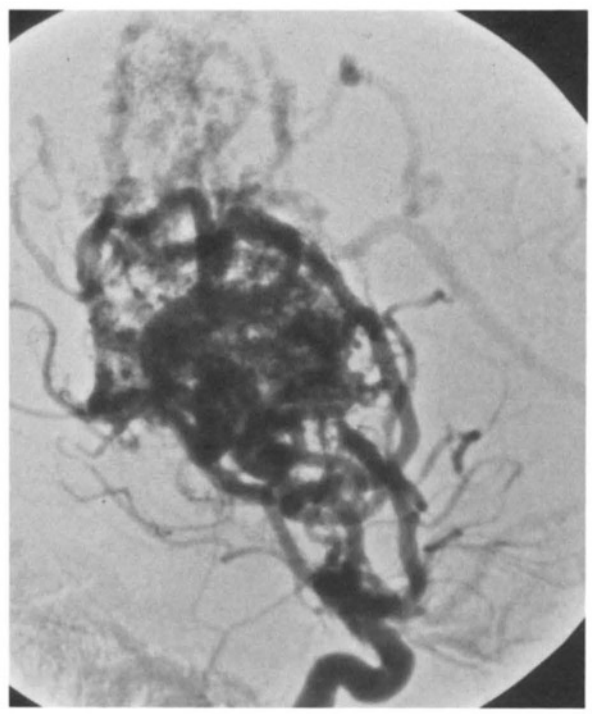

D

Fig 1. Left internal carotid angiogram, lateral projection in 4 patients with arteriovenous malformations. Note: Disc electrodes used for monitoring during embolization or superselective amobarbital testing are visible. (A) Patient 1. (B) Patient 2, after intraoperative embolization. (C) Patient 3. (D) Patient 4.

itor (Macintosh II cx, Apple Computers, Cupertino, CA). The monitor was placed directly in front of the subject so that it could be touched comfortably with an outstretched arm. The target was 0.5 cm in diameter and moved randomly within a fixed window of 6 × 8 cm. Target velocity was 6 cm/sec and changed direction on average 200 times/min. For control studies, the subject was instructed to follow the movement of the target with their eyes only. Peripheral vision was shielded to eliminate visual distraction.

For index finger tracking, the subjects were instructed to track the moving target with the index finger of the dominant hand. The axis of rotation was about the first metacarpophalangeal joint. For this task the video monitor was lightly touched. The subjects practiced the tracking until only the

first finger slid gently over the target and without any jumping movement. Normal subjects used the dominant hand (10 right-handed, 2 left-handed) whereas all 4 AVM patients used the right hand, contralateral to the AVM (Patients 1, 2, and 4 with dominant right hand and Patient 3 with nondominant right hand).

Some of the subjects performed other somatotopic tasks. In an arm tracking task, the dominant hand was held lightly in a fist and pointed at the same target. The axis of rotation during target tracking was at the shoulder. In a third motor paradigm the subject followed the moving target with the great toe of the dominant side. The leg was completely relaxed at the hip and knee and lay in extension. Dorsiflexion of the toe and rotation at the ankle allowed for accurate tracking. In the last tracking test, the subjects followed the target with their tongue extended. They were coached not to use their lips, face, or limbs in concert with the tongue movement.

Each task was performed for 2 minutes beginning with the injection of radioactive water and simultaneous dynamic PET. Subjects were monitored by visual inspection for any axial or appendicular movements other than those of the designated limb or digit.

Image Analysis: First, errors secondary to image misalignment because of head movement occurring between scans were removed with an automated algorithm [19]. In the AVM patients, the relative counts within the AVM that were greater than those in the normal cortex were masked digitally. Then, edited images from each subject were normalized to a common global value so that the AVM flow values would not affect the normalization calculation. Pixel by pixel subtractions of the edited and normalized images were then calculated. The percent change in relCBF images was evaluated using the Sun 4/60 computer (Sun Microsystems, Cupertino, CA) and the Analyze program (Mayo Clinic, Rochester, MN). The spatial location and magnitude of the maximum response in the right and left primary motor cortices, supplementary motor area (SMA), and right ipsilateral anterior superior cerebellum were measured for each task in each individual. The magnitude of a relCBF response was assumed to be proportional to the local neuronal activity [20]. In two previous studies we showed the above sites to demonstrate consistent, significant responses both within and across subjects during visually guided motor tracking tasks [17, 18]. From previous reproducibility studies, the within-subject coefficient of variation for the magnitude of response in the primary motor cortex, cerebellum, and SMA was determined to be 9%. The variability of the spatial location of the motor cortex peak response in normal subjects was measured after correction for any head movements and was found to be less than 3 mm (2 pixels) in any direction.

Response localization was determined with respect to two anatomical references. In the first, the PET and MRI scans were matched and registered in a standardized fashion as previously described [17, 18]. The PET percent change images were then superimposed on MRIs to confirm response site localization.

In the second anatomical reference, each percent change image was resliced to generate a 2.5-cm-thick coronal section that passed through the dorsal to ventral extent of the central fissure as previously described [17]. From this section, a midline point at the roof of the third ventricle was identified. A radial from this point to each maximum in the motor cortex was generated. The solid angle that this radial formed, relative to the midline, could then be determined and compared with that of a normal population.

Results from the 2 left-handed control subjects were reversed so that the greatest relCBF response, contralateral to the performing limb, would be located in the left side of the brain. Thus, results for all control subjects would be greatest in the left hemisphere to facilitate comparison with the 4 AVM patients.

Results

Three of the 4 patients demonstrated well-defined relCBF responses in the bilateral primary motor cortices, SMA, and ipsilateral anterior cerebellum, similar in location to those of the normal control population. In the only subject with a significant right arm paresis (Patient 4), there was an attenuation of the relCBF response in the left primary motor cortex and an absence of a response in the cerebellum. In all of the patients, the augmentation of blood flow in the contralateral primary motor cortex, adjacent to each AVM, could be clearly distinguished from the blood flow of the malformation itself, as demonstrated in Figure 2. Localization in the motor cortex followed the classic homuncular representation that was identified in a normal subject using the same methodology [17]. There were no novel foci of relCBF in the primary motor cortex to suggest an unusual redistribution of somatotopy. Two patients (Patients 1, 3) had also undergone intraoperative cortical mapping of the postcentral gyrus hand area with median nerve somatosensory stimulation. With both intraoperative photographs and angiograms, location of the somatosensory hand area was estimated by determining the distance along the primary fissure from the interhemispheric fissure to the site of maximal physiological response. There was approximate concordance across the central fissure between the physiological estimate of the sensory hand area derived from median nerve stimulation and the motor hand area determined by the site of maximal relCBF response measured with PET.

The site of each primary motor cortex response was also examined in the coronal perspective. The angular displacement for which a response was located relative to the third ventricle is demonstrated in Figure 3. The patient with the largest frontal AVM (Patient 1) demonstrated displacements of finger, arm, and tongue responses that were superior to

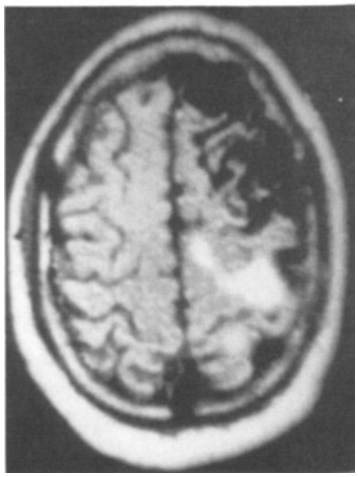

A

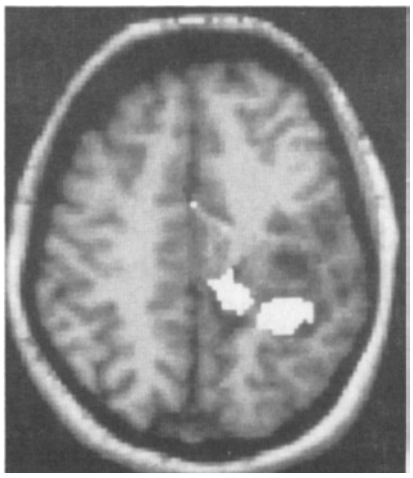

D

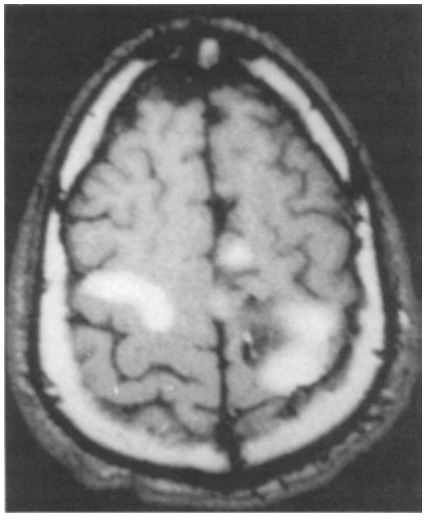

B

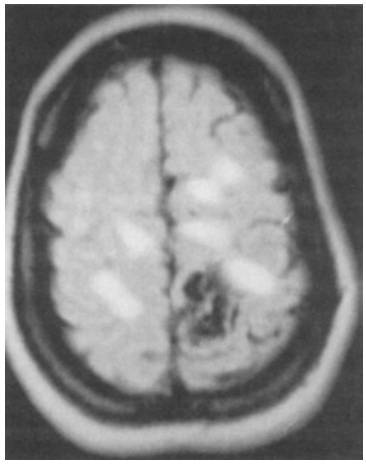

C

Fig 2. Functional localization of PET responses during right index finger tracking in 4 patients with arteriovenous malformations (AVMs). Patients 1 through 4 are shown in order in images (A) through (D). In each, positive PET relative cerebral blood flow (relCBF) responses of more than 5% (in white) have been superimposed on the same subject's MRI. Axial sections at the level of the hand area in the primary cortex are shown. Each shows a left primary motor cortex on the right side of the image and supplementary motor area response near the midline. Note the close proximity of the left primary motor cortex relCBF response adjacent to the AVM in each patient. The right primary motor cortex response, of lesser magnitude, is also visible in Patients 2 and 3. In Patients 1 and 4 it was located on another section and is not visible in this plane.

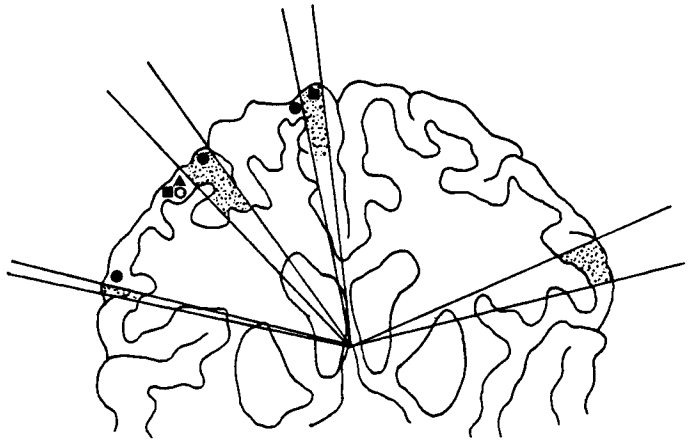

Fig 3. Solid angles representing a 95% confidence interval (CI) within which the maximal site of activation of the primary motor cortex would be expected to occur for movements of the contralateral toe (mean: 83.5; 95% CI: 80.7–86.3), contralateral tongue (mean: 14.8; 95% CI: 14.0–15.6), ipsilateral tongue (mean: 16.8; 95% CI: 12.0–21.7), and contralateral finger (mean: 53.0; 95% CI: 49.4–56.6). Angles from the population have been projected onto a coronal section from one of the normal subjects that passes through the primary motor cortex. Responses from the 4 patients with arteriovenous malformations have been superimposed. Solid circles = Patient 1; squares = Patient 2; triangle = Patient 3; open circle = Patient 4.

those of the control population. This abnormality could be accounted for by the large size of the AVM and associated distortion of global brain anatomy. The remaining 3 patients demonstrated responses in a normal location.

The magnitude of relCBF responses in the 4 patients with AVMs are summarized in the Table. For 3 patients (Patients 1–3), responses in the contralateral motor cortex, adjacent to the AVM, were within normal limits. RelCBF responses in the primary motor cortex ipsilateral to the performing limb were significantly increased as they were outside the 95% confidence interval for inclusion in the control group. The contralateral motor cortex response was below normal in 1 patient (Patient 4) who had a right arm paresis. All 4 AVM patients also demonstrated augmentation of relCBF in the SMA that was greater than expected based on the control population estimates. Responses in the cerebellum were normal for Patients 1 and 3, increased in Patient 2, and absent in Patient 4.

Discussion

This study demonstrated that the functional anatomy of the human motor system can be noninvasively mapped by PET in patients who have large AVMs adjacent to the motor strip. The PET images are straightforward to acquire, analyze, and coregister with MRI structural information. The location of the relCBF responses within the primary motor cortex is concordant with the known somatotopic organization of the precentral gyrus. In addition, there was approximate agreement in the location of the precentral motor hand area as determined by PET and the postcentral sensory hand areas located by direct cortical mapping in Patients 1 and 3. These results are complementary to those from a previously reported PET mapping strategy that defined the hand area of the postcentral gyrus using passive vibrotactile stimulation in a single individual [11]. In that patient, the CBF response in the sensory cortex matched the site localized by direct cortical mapping. From these two different studies it can be concluded that PET mapping can be tailored to individual patients to map either the sensory or the motor systems, contingent on the exact location of an AVM relative to the central sulcus.

It is important to note that in these 4 patients, the results of functional mapping by PET were not primarily used to decide on a recommendation for treatment. Management decision making was based on the results of conventional imaging studies. In each subject the results of PET motor cortex localization were consistent with and reinforced the results of the standard techniques. The results of this study suggest that superimposition of the PET response sites on matching MRIs provides an accurate, detailed functional localization map that can be used to select among and plan for a variety of management choices. These would include surgical resection, embolization, stereotaxic radiosurgery, and conservative therapy [3, 21].

Despite the presence of an AVM adjacent to the motor cortex, significant redistribution of the motor cortex responses was not observed. That is, there was no measurable evidence for relocation of the CBF response for the hand area within the primary motor cortex to suggest massive (>1 cm) somatotopic reorganization. Although the image resolution of the PET CBF images was higher than 13 mm, the ability to detect a shift in the location of a solitary CBF response in the percent change image is proportional to the image pixel size of 1.75 mm. Thus, even with moderately low-resolution images it can be possible to detect very small shifts in the location of the maximum of a solitary response [22]. Large-scale reorganization was demonstrated in the primary sensory cortex of nonhuman primates after long-term peripheral deafferentation [23]. However, operative experience in humans would suggest that spatial reorganization may not occur until the cortex is directly involved. The lack of relocation in the present study may be due to insufficient disruption of the motor cortex projections by the AVMs.

Other components of the motor system that are active in normal subjects were also active in the 3 AVM patients with preserved motor function of the arm. Within this system, there was an increase of relCBF noted in the SMA and the primary motor cortex ipsilateral to the hand performing the task in all 4 AVM patients. A strategy of using PET changes of absolute CBF was previously used to identify cerebral adaptation in patients recovering from stroke [24]. In that study, the principal finding was an augmentation of CBF in the opposite (uninjured) motor cortex after functional recovery. One interpretation of this phenomenon is that the increased activity in the ipsilateral hemisphere might represent cerebral plasticity. Changes in the AVM patients might also

Relative Cerebral Blood Flow (CBF) Responses During Right Index Finger Tracking[a]

Patient No.	Motor Cortex		Supplementary Motor Area	Anterior Cerebellum (Right)
	Left	Right		
1	45	34[b]	25[b]	31
2	41	35[b]	22[b]	50
3	38	24[b]	22[b]	31
4	26	18	22	Absent
Normals[c]	35 (29–42)	17 (12–22)	16 (12–19)	33 (26–39)

[a] Values are peak percent increase of relative CBF during right index finger movements compared to a control scan of eye movements.
[b] Value is outside of 95% confidence interval for inclusion in control group.
[c] 95% confidence interval for control group.

represent cerebral plasticity; however, the results should be considered as preliminary given the small number of subjects and the methodological assumptions that were employed. A larger series of AVM subjects with absolute measures of CBF will be required to use a similar strategy to identify adaptation based on changes of CBF magnitude. Only in Patient 4, who alone had impaired right arm movements, was the CBF response of the left motor cortex below normal. This may be due to neuronal dropout in motor cortex from compressive or ischemic damage caused by the AVM, or to an abnormality in the behavior-induced vascular response secondary to the hemodynamic effect (''steal'') of the AVM [16]. This patient also failed to show augmentation of activity in the right motor cortex and anterior cerebellum. This AVM may be interrupting corticopontocerebellar pathways in addition to corticospinal tracts.

The present results reveal that patients with large AVMs and preserved motor function continue to maintain typical vascular responses in adjacent functional cortex despite the presence of a profound focal blood flow disturbance in the nidus of a vascular malformation. Because of this preservation of local CBF responses, PET can be used as a valuable adjunct for the mapping of viable cortical function in the region of the central sulcus. The magnitude of the CBF response is robust, raising the possibility of mapping the motor cortex with new nonradioactive imaging techniques such as functional MRI. Further developments in the design of PET neurobehavioral paradigms may provide a complete repertoire of tasks for determining the functional integrity of neocortex in any part of the cerebrum disrupted by an AVM.

This work was supported in part by Department of Energy cooperative agreement DE-FC03-87ER60615 and National Institute of Mental Health grant RO1-MH-37916.

The authors wish to acknowledge D. K. Mahoney, O. Ratib, G. Porenta, and W. Kuhle for software development, and to Lee Griswold for preparation of illustrations.

References

1. Ondra SL, Troup H, George ED, Schwab K. The natural history of symptomatic malformations of the brain: a 24 year follow-up assessment. J Neurosurg 1990;73:387–391
2. Spetzler R, Martin NA. A proposed grading system for arteriovenous malformations. J Neurosurg 1986;65:476–483
3. Steinberg GK, Fabrikant JI, Marks MP, et al. Stereotactic heavy-charged-particle Bragg-peak radiation for intracranial arteriovenous malformations. N Engl J Med 1990;323:96–101
4. Martin N, Grafton S, Vinuela F, et al. Imaging techniques for cortical functional localization. In: Clinical neurosurgery. New York: Raven, 1992:132–165
5. Penfield W, Boldrey E. Somatic motor and sensory representation in the cerebral cortex of man as studied by electrical stimulation. Brain 1938;15:389–443
6. Burchiel KJ, Clarke H, Ojemann GA, et al. Use of stimulation mapping and corticography in the excision of arteriovenous malformations in sensorimotor cortex and language-related neocortex. Neurosurgery 1989;24:322–327
7. Wood CC, Spencer DD, Allison T, et al. Localization of human sensorimotor cortex during surgery by cortical surface recording of somatosensory evoked potentials. J Neurosurg 1988;68:99–111
8. Rauch R, Vinuela F, Dion J, et al. Pre-embolization functional evaluation in brain AVMs. Part I: the superselective Amytal test. AJNR 1992;13:303–308
9. Rauch R, Vinuela F, Dion J, et al. Pre-embolization functional evaluation in brain AVMs. Part II: the ability of superselective Amytal test to predict neurological dysfunction before embolization. AJNR 1992;13:309–314
10. Berger M, Cohen W, Ojemann G. Correlation of motor cortex brain mapping with magnetic resonance imaging. J Neurosurg 1990;72:383–387
11. LeBlanc R, Meyer E. Functional PET scanning in the assessment of cerebral arteriovenous malformations. Case report. J Neurosurg 1990;73:615–619
12. Herscovitch P, Markham J, Raichle ME. Brain blood flow measured with intravenous $H_2{}^{15}O$. I. Theory and error analysis. J Nucl Med 1983;24:782–789
13. Raichle ME, Martin WRW, Herscovitch P. Brain blood flow measured with intravenous $H_2{}^{15}O$. II. Implementation and validation. J Nucl Med 1983;24:790–798
14. Fox PT, Mintun MA, Raichle ME, Herscovitch P. A non-invasive approach to quantitative functional brain mapping with $H_2{}^{15}O$ and positron emission tomography. J Cereb Blood Flow Metab 1984;4:329–333
15. Mazziotta JC, Huang S-C, Phelps ME, et al. A noninvasive positron computed tomography technique using oxygen-15-labeled water for the evaluation of neurobehavioral task batteries. J Cereb Blood Flow Metab 1985;5:70–78
16. Tyler JL, Leblanc R, Meyer E, et al. Hemodynamic and metabolic effects of cerebral arteriovenous malformations studied by positron emission tomography. Stroke 1989;20:890–898
17. Grafton ST, Woods RP, Mazziotta JC, Phelps ME. Somatotopic mapping of the primary motor cortex in man: activation studies with cerebral blood flow and PET. J Neurophysiol 1991;66:735–743
18. Grafton ST, Mazziotta JC, Woods RP, Phelps ME. Human functional anatomy of visually guided finger movements. Brain 1992;115:565–587
19. Woods RP, Cherry SR, Mazziotta JC. Rapid automated algorithm for aligning and reslicing PET images. J Comput Assist Tomogr 1992;115:565–587
20. Fox PT, Raichle ME. Stimulus rate determines regional brain blood flow in striate cortex. Ann Neurol 1985;17:303–305
21. Kjellberg RN, Hanamura T, Davis KR, et al. Bragg-peak proton-beam therapy for arteriovenous malformations of the brain. N Engl J Med 1983;309:269–274
22. Fox PT, Mintun MA, Raichle ME, et al. Mapping human visual cortex with positron emission tomography. Nature 1986;323:806–809
23. Pons TP, Garraghty PE, Ommaya AK, et al. Massive cortical reorganization after sensory deafferentation in adult macaques. Science 1991;252:1857–1860
24. Chollet F, DiPiero V, Wise RJS, et al. The functional anatomy of motor recovery after stroke in humans: a study with positron emission tomography. Ann Neurol 1991;29:63–71